Cell, Vol. 100, 265–276, January 21, 2000, Copyright ©2000 by Cell Press

E. coli Hemolysin E (HlyE, ClyA, SheA): X-Ray Crystal Structure of the Toxin and Observation of Membrane Pores by Electron Microscopy

Alistair J. Wallace, Timothy J. Stillman, Angela Atkins, Stuart J. Jamieson, Per A. Bullough, Jeffrey Green, and Peter J. Artymiuk*
The Krebs Institute
Department of Molecular Biology and Biotechnology
University of Sheffield, Western Bank
Sheffield S10 2TN
United Kingdom

Summary

Hemolysin E (HlyE) is a novel pore-forming toxin of *Escherichia coli*, *Salmonella typhi*, and *Shigella flexneri*. Here we report the X-ray crystal structure of the water-soluble form of *E. coli* HlyE at 2.0 Å resolution and the visualization of the lipid-associated form of the toxin in projection at low resolution by electron microscopy. The crystal structure reveals HlyE to be the first member of a new family of toxin structures, consisting of an elaborated helical bundle some 100 Å long. The electron micrographs show how HlyE oligomerizes in the presence of lipid to form transmembrane pores. Taken together, the data from these two structural techniques allow us to propose a simple model for the structure of the pore and for membrane interaction.

Introduction

Recent outbreaks of *Escherichia coli*–associated food poisoning have emphasized the importance of identifying and characterizing the various virulence factors of this organism. This paper reports the structure of a recently discovered novel *E. coli* toxin, variously named hemolysin E (HlyE) (Green and Baldwin, 1997; Reingold et al., 1999), cytolysin A (ClyA) (Oscarsson et al., 1996), or silent hemolysin A (SheA) (Ludwig et al., 1995). This structure represents the first member of a new family of pore-forming toxins, which are also found in other pathogenic organisms, including species of *Salmonella* and *Shigella* (Figure 1).

HlyE is unrelated to the well-characterized pore-forming *E. coli* hemolysins of the RTX family (Coote, 1992), hemolysin A (HlyA) (O'Brien and Holmes, 1996), and the enterohemolysin encoded by the plasmid borne *ehxA* gene of *E. coli* 0157 (Bauer and Welch, 1996). However, it is evident that expression of HlyE in the absence of the RTX toxins is sufficient to give a hemolytic phenotype in *E. coli* (Ralph et al., 1998), and hemolytic avian *E. coli* isolates have been reported that lack the RTX toxins but possess a close homolog of HlyE (Reingold et al., 1999) (Figure 1), and that HlyE is present in pathogenic strains of *E. coli*, including *E. coli* 0157 (del Castillo et al., 1997). It is a protein of 34 kDa that is expressed during anaerobic growth of *E. coli* (Green and Baldwin, 1997; Ludwig et al., 1999). Anaerobic expression is controlled by the transcription factor, FNR, such that, upon ingestion and entry into the anaerobic mammalian intestine, HlyE is produced and may then contribute to the colonization of the host (Green and Baldwin, 1997). Unlike HlyA, which is synthesized as a soluble protoxin that requires proteolytic processing and posttranslational acylation to produce the active toxin (Stanley et al., 1994), HlyE requires no posttranslational processing (del Castillo et al., 1997; Ludwig et al., 1999). Previous comparisons of the *hlyE* sequence against the available databases had revealed no similarity to any other known hemolysin or characterized gene product. However, Southern blotting studies had indicated that DNA capable of hybridizing to a *hlyE* probe is present in all the strains of *E. coli* tested, including 0157, as well as *Shigella flexneri*, but not *Salmonella* D9 (del Castillo et al., 1997). Sequence comparisons reported here confirm that the typhoid fever–causing bacterium *Salmonella typhi* and the dysentery-causing organism *Shigella flexneri* have highly homologous proteins to HlyE encoded in their genomes (Figure 1). These observations suggest that there is a family of HlyE-like hemolysins and that they are likely to be a significant component of these pathogens' armory of toxins.

Osmotic protection assays and lipid bilayer experiments show that HlyE forms a moderately cation-selective water-permeable pore of diameter 25–30 Å (Ludwig et al., 1995, 1999; Oscarsson et al., 1999). It is thought that HlyE pore formation is either part of a mechanism for iron acquisition by the bacterial cell (del Castillo et al., 1997) or that it may promote bacterial infection by killing immune cells and causing tissue damage (Ludwig et al., 1999). On the basis of hydrophobocity calculations, HlyE has been predicted to have one putative transmembrane segment ranging from residues 177 to 203 (Figure 1); in addition, there is a second shorter hydrophobic sequence from residues 89 to 101 (del Castillo et al., 1997).

This paper reports the three-dimensional structure determination of HlyE from *E. coli* K12 in its putative water-soluble secreted form and the first observations of pore formation in lipid vesicles by electron microscopy. These investigations reveal how HlyE folds and the nature of its association to form pores in the membranes of cells.

Results

Structure Solution by X-Ray Crystallography at 2.0 Å Resolution

HlyE for crystallization was prepared from a GST-HlyE fusion protein containing a thrombin cleavage site and overexpressed in *E. coli*. The sequence of the crystallized protein consists of the whole sequence of HlyE preceded by a 15-residue linker peptide, a construct that has hemolytic properties in vitro that are indistinguishable from the wild-type protein. Crystals of HlyE

*To whom correspondence should be addressed (e-mail: p.artymiuk@sheffield.ac.uk).

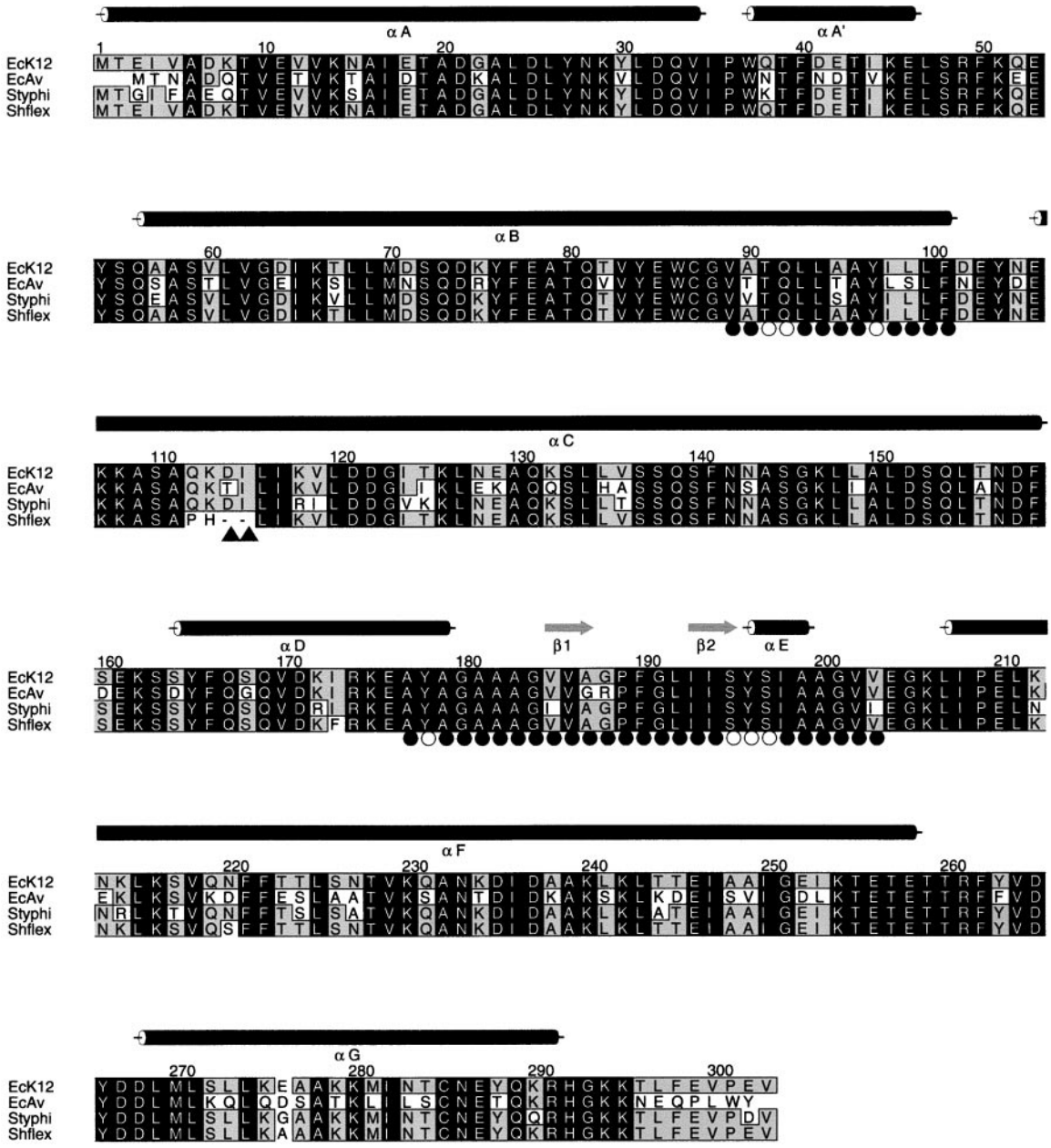

Figure 1. Sequence Alignments of HlyE Toxin Family

The four currently known hemolysin sequences from *E. coli* K12 (EcK12), avian *E. coli* (EcAv), *Salmonella typhi* (Styphi), and *Shigella flexneri* (Shflex) are shown. Conserved residues are shown in white letters on a black background, residues identical in only two or three sequences as black letters on a grey background, all others as black letters on white background. Cylinders and arrows above the sequences indicate the positions of helices and strands respectively in the *E. coli* K12 HlyE structure. The proposed transmembrane region (residues 177 to 203) is underlined by a row of circles, filled for hydrophobic, empty for hydrophilic residues in the *E. coli* K12 sequence. The two filled triangles indicate the point at which the sequence of the *Shigella flexneri* gene has an 11 bp deletion. This causes the premature termination of the encoded protein by introducing a stop codon at this position. The sequence downstream of the deletion can be translated as indicated, and although it is unlikely in this strain (ATCC 12022) that this portion of the protein will be produced in vivo, it serves to illustrate the conserved regions of HlyE. Diagram produced using ALSCRIPT (Barton, 1993).

were grown from ammonium sulfate solutions in space group $P4_32_12$, with cell dimensions a = b = 87.4 Å, c = 143.6 Å, and with one molecule in the asymmetric unit. These crystals diffracted to 2.56 Å at room temperature, and the structure was solved at that resolution by multiple isomorphous replacement (MIR) using three heavy atom derivatives (Table 1A). The model was refined to a working crystallographic R factor of 0.199 at 2.56 Å. Next, cryogenic conditions were developed that enabled data to be collected to 2.0 Å, and the structure was refined to an R factor of 0.198 at that resolution (Table 1B). Although the cryo-cooled crystals have somewhat

Table 1. Data Collection, MIR Phasing, 2 Å Model Refinement Statistics, and Mutagenesis Data

(A) Data Processing and Heavy Atom Statistics

Dataset	Native 1	Native 2	Combined 1 and 2	Native (cryo)	EMP	PCMBS	$K_2Pt(Cl)_4$	$KAuCl_4$	$UO_2(Ac)_2$
Resolution (Å)	12.6–2.7	28.4–2.56	28.4–2.56	17.8–2.0	16.7–3.0	23.7–2.5	23.6–3.5	23.7–3.5	24.0–3.5
Beamline[a]	DL P.X 9.5	DL P.X 9.6	—	DL P.X 7.2	SHEF	DL P.X 9.6	SHEF	SHEF	SHEF
Detector	MAR 3000	MAR 345	—	MAR 345	MAR 345	CCD	MAR 345	MAR 345	MAR 345
Wavelength (Å)	0.900	0.870	—	1.488	1.540	0.870	1.540	1.540	1.540
Observed/unique refls.	55,774/12,933	23,891/14,612	84,732/17,680	78,696/31,955	44,672/10,806	38,372/14,044	48,188/7,188	48,567/7,219	42,611/7,114
R_{merge} (%)[b]	6.4 (35.1)	3.9 (17.3)	9.5 (17.2)	3.6 (5.6)	8.6 (27.4)	4.6 (30.3)	11.5 (28.9)	12.1 (27.2)	11.5 (24.5)
Completeness (%)[b]	82.1 (44.8)	81.0 (84.4)	95.9 (84.4)	89.3 (72.0)	93.4 (96.0)	73.8 (76.5)	96.1 (100.0)	96.5 (100.0)	95.1 (100.0)
I/σ[b]	10.9 (2.2)	13.3 (3.3)	5.5 (3.3)	12.0 (7.6)	6.7 (2.8)	11.2 (2.0)	6.3 (2.6)	6.0 (2.8)	6.3 (3.0)
[Heavy atom] (mM)	—	—	—	—	1	1	1	1	1
No. of sites	—	—	—	—	2	1	2	3	5
R_{iso} (%)	—	—	—	39.3	24.1	21.3	15.7	13.8	14.1
Phasing power 6 Å	—	—	—	—	1.86 (1.21)	2.66 (1.73)	1.43 (1.03)	2.96 (2.28)	1.21 (0.81)
R_{cullis} 6 Å	—	—	—	—	0.63 (0.72)	0.50 (0.57)	0.75 (0.69)	0.48 (0.42)	0.80 (0.80)
Phasing power 2.6 Å	—	—	—	—	1.28 (0.87)	1.65 (1.11)	—	1.57 (1.22)	—
R_{cullis} 2.6 Å	—	—	—	—	0.77 (0.85)	0.70 (0.76)	—	0.72 (0.64)	—

(B) Refinement Statistics

Resolution range (Å)	17.6–2.0
Sigma cutoff	none
Number of reflections (working/free sets)	29,924/1,586
Number of atoms (protein/other)	2,371/344
R_{work}/R_{free}	0.198/0.252
RMS deviation from ideality:	
Bond lengths	0.011 Å
Bond angles	1.7°
Dihedral angles	15.1°
RMS deviation of B factors of bonded atoms:	
overall	5.25 $Å^2$
main chain	3.46 $Å^2$
side chain	7.34 $Å^2$
Ramachandran plot. Proportion of residues in:	
allowed regions	96.8%
additional allowed regions	3.2%
disallowed regions	0.0%
Average B factors (main chain/side chain)	24/32 $Å^2$
Number of waters/average B factor	339/39 $Å^2$
Number of sulfates/average B factor	1/44 $Å^2$

(*continued*)

Table 1. Continued

(C) Mutagenesis Data

Variant	Hemolytic Activity (HU mg^{-1})[c]	Half-Life (min) (at 42°C)
HlyE wild type	1×10^6	4.7
GST-HlyE	9×10^4	ND
HlyE-C87S	7×10^5	2.2
HlyE-C285S	4×10^5	0.9
HlyE-V185S, A187S, I193S	21	ND

$R_{merge} = \Sigma||I - <I>|/\Sigma I$, where I is the integrated intensity of a given reflection. $R_{iso} = \Sigma|F_{PH} - F_P|/\Sigma F_P$, where F_{PH} and F_P are the derivative and combined 1 and 2 native structure factor amplitudes. Phasing power = <rms heavy atom structure factor>/<rms lack of closure> for acentric reflections (values for centric relections given in parentheses). R_{cullis} = <rms lack of closure>/<rms isomorphous difference> for acentric reflections (values for centric relections given in parentheses). EMP, ethylmercury phosphate ($C_2H_5HgPO_4$). PCMBS, 4-(chloromercuri) benzene sulphonic acid sodium salt ($ClHgC_6H_4SO_3Na$). $UO_2(Ac)_2$, uranyl acetate ($UO_2(OCOCH_3)_2$). $R_{work} = \Sigma||F(obs)| - |F(calc)||/\Sigma|F(obs)|$ for the 95% of the reflection data used in refinement. $R_{free} = \Sigma||F(obs)| - |F(calc)||/\Sigma|F(obs)|$ for the remaining 5%. ND, not determined.

[a] DL, at CCLRC Daresbury Laboratories Synchrotron Radiation Source stations P.X 9.5, P.X 9.6, and P.X 7.2; SHEF, on a MAR345 detector/Rigaku RU200 rotating anode generator at University of Sheffield.

of the reflection data excluded from the refinement.

[b] Values for the outermost resolution shell are given in parentheses.

[c] HU, hemolysin units per mg HlyE protein (Rowe and Welch, 1994).

different cell dimensions (a = b = 84.5 Å, c = 142.7 Å) and the mean isomorphous difference is large (0.39), the structures are virtually identical on superposition (root-mean-square deviation on Cα's of 0.56 Å), and it is the 2.0 Å resolution structure that is reported here.

Description of Structure

HlyE is a long, rod-shaped molecule, with approximate dimensions 100 Å × 30 Å × 20 Å. The shaft of the rod is formed by a bundle of four helices, each 70–80 Å long: A/A′ (residues 1–34 and 37–46, with a distinct kink at residues 35–36), B (56–101), C (106–159), and F (207–258). These four helices are arranged with a simple square, left-handed, up-down-up-down topology (Presnell and Cohen, 1989; Harris et al., 1994), as shown in Figures 2A and 2C. Except for the discretely kinked A/A′ helix, the helices coil gently around each other in a left-handed supercoil whose center consists almost entirely of hydrophobic side chains.

However, at each end of the rod there are significant elaborations to this simple structure. First, at the lower end of the bundle, 24 residues (268–291) from the C-terminal region fold to make an additional 35 Å long helix (Figures 2A and 2D). This helix (helix G) packs between helices A and B, so as to form a five-helix bundle for about one-third of the length of the molecule. This "tail" subdomain has an unusual topology that does not occur elsewhere in the Protein Data Bank (Bernstein et al., 1977), as confirmed by database searches (Grindley et al., 1993). The second unusual structure occurs at the other extremity of the molecule, where an additional subdomain (Figures 2A and 2B) is located between the third and fourth helices of the main bundle. This "head" subdomain consists of a short β hairpin (the "β tongue") flanked by two short helices of 16 and 4 residues respectively (helices D and E). This subdomain is of extreme interest as the β tongue is located within the predicted transmembrane region (del Castillo et al., 1997), as discussed below.

These major secondary structures are linked by short stretches of random coil that sometimes include additional short helical segments, giving a molecule that overall is 81% helix and 2% β strand. Almost the entire chain is well ordered and distinct in the electron density maps except for the last 5 residues at the C terminus. The true N terminus of native HlyE (Met 1) is well ordered, as are the final 5 residues of the preceding linker region (residues −4 to 0), which fold in helical conformation as an N-terminal extension to helix A. However, the first 10 residues of the 15-residue linker from the cleaved GST fusion cannot be seen in the electron density map.

Similarities to Other Protein Structures

Although the underlying four-helix bundle topology is very common and found in a wide variety of proteins (Harris et al., 1994), the length of the helices in the bundle coupled with the two additional structural features, namely the "head" subdomain and the fifth helix in the "tail" subdomain, lead to the conclusion that HlyE possesses a novel fold, as confirmed by structural database searches (Grindley et al., 1993).

Nevertheless, some analogies with other toxins and membrane-associated proteins can be drawn. First, the overall elongated shape of the molecule is reminiscent

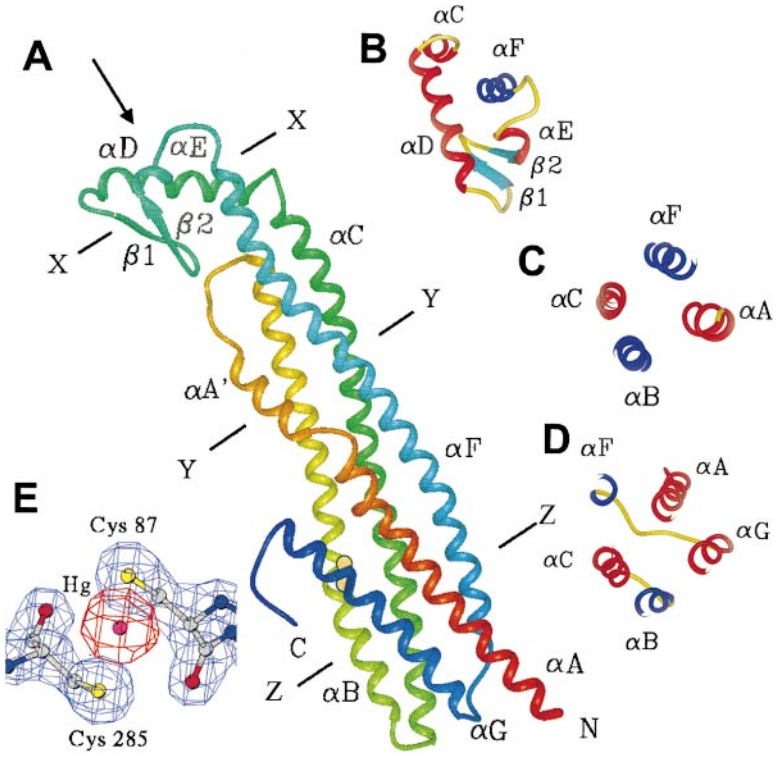

Figure 2. The Fold of HlyE

(A) The overall fold of *E. coli* HlyE is shown as a main chain ribbon colored from red to blue, from the N to C termini. The two cysteine residues are represented as yellow circles. Three cross sections are indicated, X-X, Y-Y, and Z-Z, and when the molecule is viewed from the direction shown by the arrow at top left, the arrangement of the helices in these three planes can be seen in (B), (C), and (D), respectively. The helices are colored red if the peptide chain is running out of the plane of the paper toward the viewer, and blue if it is leading away. Connecting loops are indicated in yellow and β strands are shown as cyan arrows. Figures were generated using MIDAS (Ferrin et al., 1988). (E) A portion of the final 2.0 Å ($2F_{obs} - F_{calc}$) exp *i*αcalc electron density map in the region of the two cysteine residues (87 and 285). The density is contoured at 1.5σ and shown as a blue mesh. Superimposed on this is the 2.5 Å difference electron density for the ethyl mercury phosphate derivative, contoured at 25σ and shown in red. This clearly indicates the presence of a mercury atom between these two cysteine residues.

of the aqueous forms of other pore-forming toxins such as aerolysin (Parker et al., 1994), perfringolysin (Rossjohn et al., 1997), and staphylococcal LukF (Olson et al., 1999), although these are based on β sheet rather than α-helical architectures. Domains involving very long helical regions are found in a number of other toxin structures, most spectacularly in colicin Ia, which contains two 200 Å–long helices (Wiener et al., 1997). Such toxin helical domains often appear to be involved in translocation across membranes, and a number of instances of this are given below in the discussion of the model for pore formation. It is also noteworthy that many other membrane-associated proteins involved in membrane fusion and/or pore formation consist of long helical coiled coils. Such proteins range from influenza virus hemagglutinin (Wilson et al., 1981) to mammalian SNARE proteins (Fernandez et al., 1998; Sutton et al., 1998), and a variety of models have been proposed for their membrane association (Harbury, 1998). However, none of these molecules has any detailed resemblance to HlyE, and there is no sequence or structural evidence of any evolutionary relationship between HlyE and any other protein family.

Regions of Sequence Conservation

The sequences of the avian *E. coli* HlyE and the HlyE homologs from *Shigella flexneri* and *Salmonella typhi* are shown aligned with that of *E. coli* K12 HlyE in Figure 1. These three sequences are respectively 74%, 98%, and 92% identical with that of the K12 protein, and 68% of residues are identical among all four sequences. Almost all substitutions are conservative, although this is not surprising since these organisms are all closely related (Salyers and Whitt, 1994). There are a number of nonconservative substitutions, but all except two occur on the surface of the molecule. One of these exceptions, the replacement of Tyr-288 by threonine in the avian *E. coli*, can be accommodated by simple hydrogen-bonding rearrangements. The other exception, the replacement of Gly-188 by arginine in the avian *E. coli*, would initially appear more problematic because this residue is situated just before the β turn in the hydrophobic β tongue region, which forms the major hydrophobic patch on the HlyE surface, discussed in detail below. However, there are two possible ways of accommodating this residue. First, if the arginine side chain, like Gly-188, is directed toward the interior of the molecule, it would not affect the hydrophobicity of the surface, but would require other side chain movements. Second, variations in the main chain conformation may allow the side chain to point outward: in this case the long aliphatic part of the side chain would form part of the hydrophobic surface of the β tongue, while the guanidinyl end group could reach to the hydrophilic parts of the surface beyond the β tongue.

There are only two cysteines (residues 87 and 285) in HlyE and both are conserved in all four sequences. The cysteines are positioned close enough to each other on adjacent helices to form a disulfide bond, but they do not do so (Figure 2A and 2E). Their γ-sulfhydryl atoms are separated by 4.1 Å, much larger than the 2.2 Å to be expected for a disulfide bond. Furthermore, their reduced state is confirmed by the fact that the mercury atom of the ethyl mercury phosphate derivative binds in a bridging position between the two sulfurs (Figure 2E).

Replacement of each cysteine by the similarly sized serine indicates that neither is essential for hemolytic activity but that both contribute to the thermostability of HlyE (Table 1C). After treatment with diamide (1 mM), up to 40% of HlyE acquired an intramolecular disulfide, which correlates to a similar loss of hemolytic activity,

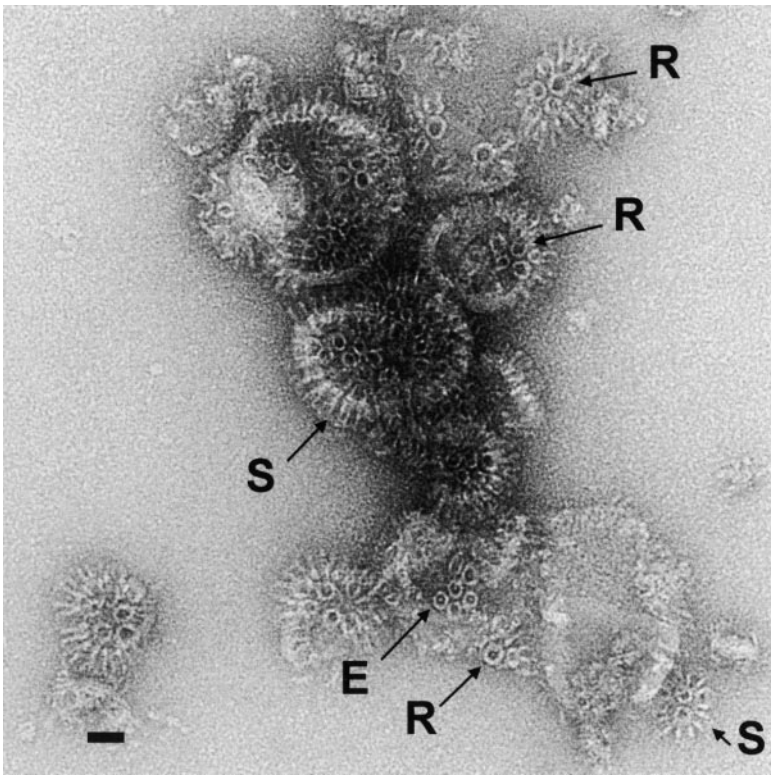

Figure 3. Electron Micrograph of HlyE in Lipid Vesicles

The micrograph shows negatively stained vesicles containing HlyE with the more heavily stained regions appearing darker. Stain-filled rings (R) are apparent in views parallel to the membrane normal. Some complexes show a central stain-excluding density (E). Side views of the protein complexes are visible at the folded edges of the vesicles as protruding spikes (S).
Scale bar (lower left) represents 200 Å.

indicating that the presence of a disulfide inhibits pore formation. Cysteines in close proximity can be characteristic of functional zinc- or iron-binding sites in proteins, but there are no other suitable side chain ligands nearby, and ICP mass spectrometry indicates that isolated HlyE is metal-free. It is unusual to encounter cysteines in an extracellular protein unless they have some other role, but what this might be, or whether there is a physiological role for any disulfide-containing form, remains unknown.

Observation of Pore Formation by Electron Microscopy

The electron micrographs of negatively stained HlyE in lipid vesicles reveal vesicles that contain numerous stain-filled ring-shaped assemblies clustered together with approximate hexagonal close packing (Figure 3). Most pores are approximately circular, although some appear to be distorted, perhaps by the sample preparation process. The majority (62%) of these assemblies appear to have an inner pore diameter of 42–52 Å and an outer diameter of 70–90 Å. However, a substantial minority (36%) of the pores are larger than this (inner diameter 55–60 Å, outer diameter 90–105 Å), and a very small number of outliers are as large as 75 Å inner and 125 Å outer diameter, perhaps indicating the existence of higher oligomeric state(s), at least in vitro. In addition to the views of pore-like structures perpendicular to the membrane plane, side views of the pore assembly can be seen as spikes protruding from the edges of the vesicles (Figure 3, arrow S). Most of these spikes are approximately 105–110 Å long separated by a 50–60 Å stain-filled gap. The thickness of the protein component is around 25–30 Å in both views. As HlyE monomers are 100 Å long and approximately 25 Å in diameter, these electron micrographs are consistent with a model for the pore in which HlyE molecules, in much the same conformation as in the crystal structure, project vertically from the membrane and pack together in a ring surrounding a channel of 50–55 Å diameter. Simple geometric calculations suggest that approximately eight HlyE molecules will be sufficient to form a pore of this size, as discussed below. However, the minority of larger pores observed suggest that larger assemblies are possible. The 50 Å pore size observed here is larger than the 25–30 Å reported from lipid bilayer experiments and from osmotic protection assays (Ludwig et al., 1995, 1999; Oscarsson et al., 1999), but there are two considerations that may limit this high value. First, because of the distribution of stain in the electron micrographs, the figure of 50 Å represents a value for the diameter of the pore at its widest point, and some of the side views suggest that the pore may have a wide vestibule that becomes more constricted as it approaches the lipid. Second, in many pore images there is evidence of exclusion of stain in the center of the ring, possibly indicative of additional mass inside the pore that may restrict the effective diameter of the pore (Figure 3, arrow E).

Orientation of HlyE in Target Membranes

It is clear from the electron micrographs that one or other pole of the HlyE molecule—either the head or the tail subdomain—must be involved in membrane association. Previous mutagenic studies indicated that the region now known to be the β tongue was required for HlyE activity (Oscarsson et al., 1999), but without the

benefit of the HlyE structure, inward-facing aspartate residues were introduced that could destroy the β tongue motif. Therefore, a HlyE variant (HlyE-V185S, A187S, I193S) was created in which three of the outward-facing hydrophobic side chains were replaced by hydrophilic serine. This variant appears to fold normally as judged by gel filtration and solubility but is essentially inactive (Table 1C), implicating the head domain in membrane association. Immunoblotting of washed erythrocyte membranes preexposed to HlyE-V185S, A187S, I193S indicated that the abolition of activity was caused by failure to associate with target membranes.

In contrast, isolated GST-HlyE retains a high level of residual pore-forming activity (~10% of wild type, Table 1C). The presence of a GST moiety at the membrane association site would be expected to severely compromise insertion into target membranes, while this result would be more consistent with mild steric hindrance of pore assembly due to the extra protein. As the GST moiety is at the N terminus of HlyE, which is in the tail domain (Figure 2A), this hemolytic activity is further evidence that it is the head, not the tail, domain that inserts into the membrane.

Therefore, in addition to the structural arguments advanced below, there is ample weight of evidence that it is the head domain containing the hydrophobic β tongue that is involved in HlyE interaction with target membranes.

Discussion

Proposed Transmembrane Region

On the basis of hydrophobicity analyses of the amino acid sequence, del Castillo et al. (1997) proposed that the most likely membrane-spanning region would comprise residues 177 to 203 (Figure 1) and that this region of the structure would be a transmembrane helix. The latter prediction is incorrect: located on the three-dimensional structure, this part of the sequence begins in the short D helix before the β hairpin, includes the whole of the β tongue and continues back into helix E (Figure 4A). This finding demonstrates that it is very dangerous to use hydrophobicity analyses as diagnostics of transmembrane helices, unless other evidence is also available. This stretch of 27 residues consists almost entirely of hydrophobic side chains (Figure 1). Some of these side chains pack internally against other parts of the molecule, but many face outwards from the β tongue and are located on the surface of the molecule (Figure 4B). In addition, two other surface residues, Phe-50 and Val-218, lie adjacent to the β tongue (Figure 4C) and further extend this hydrophobic surface region, which therefore corresponds to the major hydrophobic area on the surface of HlyE. The nonhydrophobic side chains in the putative transmembrane sequence, serines 195 and 197 and (arguably) tyrosines 178 and 196 do not compromise the hydrophobicity of the surface patch in the three-dimensional structure as they are situated at the root of the β tongue at the top of the molecule (Figure 4C), where they could in principle interact with hydrophilic lipid head groups in a membrane-bound model of the toxin.

A second, shorter hydrophobic region was also identified from sequence analysis (del Castillo et al., 1997) and corresponds to residues 89–101 at the C-terminal end of helix B (Figures 1 and 4B). In the structure, the side chains of Val-89, Ala-95, Ala-96, Ile-98, Leu-99, Leu-100, together with neighboring side chains Ile-115 (helix C) and Ile-282 (helix G), form a second hydrophobic surface patch at the lower end of the molecule. In the crystal two HlyE molecules form a head-to-tail dimeric structure that buries the two hydrophobic surface patches against each other. This involves relatively few specific contacts between the two molecules: only six direct protein:protein hydrogen bonds are made per subunit, although 1570 $Å^2$ (9.7%) of the accessible monomer surface area is buried from solvent on formation of the dimer. Although it is tempting to suggest that this dimerization may indicate a plausible strategy by which HlyE could maintain high solubility in aqueous media by sequestering the hydrophobic lipid-binding residues away from solvent (as has been observed in the water-soluble toxin proaerolysin [Parker et al., 1996]), gel filtration studies show that HlyE is a monomer in solution.

In addition to implicating what we now know to be the β tongue region in pore formation, Oscarsson et al. (1999) also proposed that residues 268–294 in the C-terminal region of HlyE, roughly corresponding to helix G in the three-dimensional structure, may also be involved in membrane targeting and pore formation. However, their arguments relied on low-level sequence resemblances between part of the C terminus of HlyE and the sequence of the short helical δ-hemolysin from *Staphylococcus aureus*. These arguments are unconvincing when the recent avian *E. coli* HlyE sequence (Reingold et al., 1999) is also considered, as this has several substitutions in helix G (Figure 1). Oscarsson et al. (1999) also showed that deletion of the last 23 residues abolished hemolytic activity completely, but since it is now clear from the structure that this involves the almost complete removal of helix G, this is likely to seriously affect the structure of the molecule rather than merely modifying activity. Moreover, the structure of HlyE reveals that the β tongue and helix G are more than 60 Å apart, and it seems most improbable that both can be directly implicated in membrane interaction.

On the basis of the mutagenic data discussed above and the structural evidence presented here and discussed in more detail below, it is evident that the large and obvious hydrophobic patch around the β tongue is the most likely site of interaction with a lipid bilayer. Moreover, its use permits the construction of the simple and conservative electron microscopy–based model for pore formation that is now described.

Model for Pore Formation

The precise mechanism of HlyE's assembly into a multimeric transmembrane pore is at present unknown. The electron microscopy results indicate that, on pore formation, HlyE forms annular oligomers, and the images are consistent with a model for an assembly in which the HlyE molecules associate with each other but retain their elongated shape, with no evidence for any drastic conformational change in the HlyE monomers. In this model the HlyE molecules are aligned normally to the membrane surface with one end of the toxin bound to the lipid, although the precise nature of the toxin's

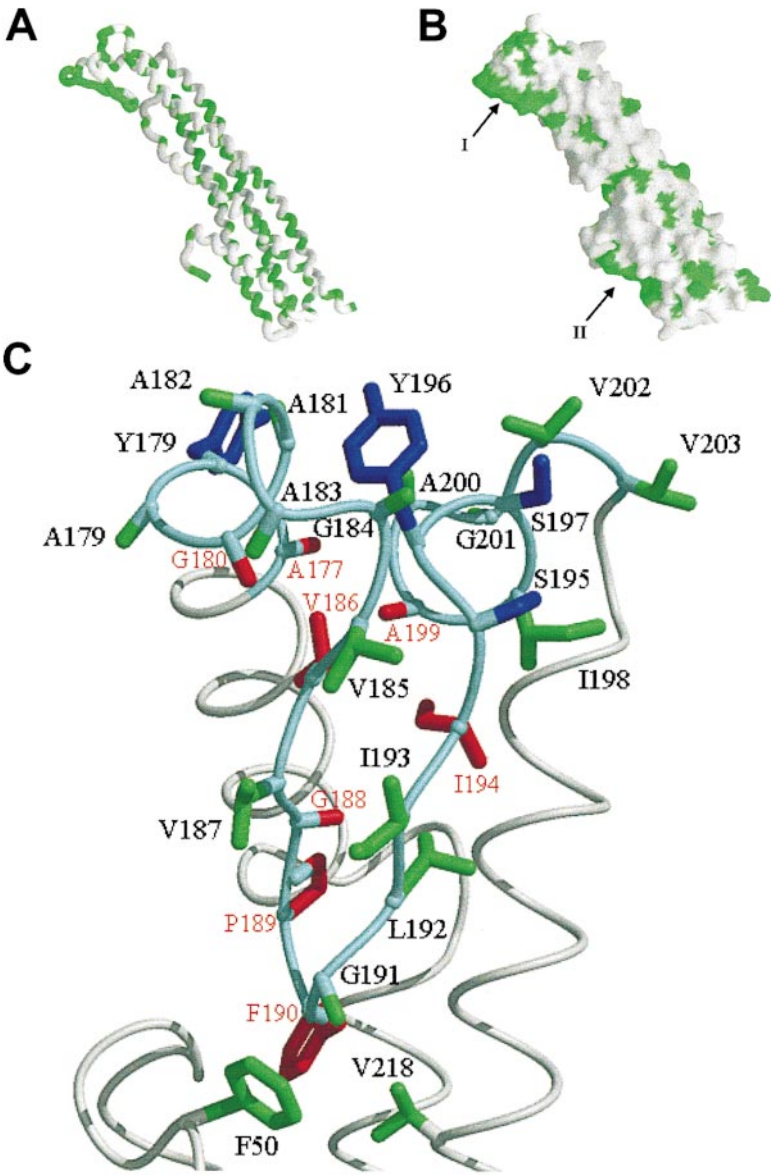

Figure 4. Hydrophobic Regions of the Structure

(A) The backbone fold of *E. coli* HlyE. Hydrophobic residues are colored green, and the others white according to the hydrophobicity scale of Eisenberg et al. (1984). Note the large number of hydrophobic residues around the β tongue region (top left).

(B) A molecular surface diagram in the same orientation as (A) and colored in the same manner, with the large hydrophobic patch indicated by I and the smaller patch by II.

(C) A detailed view of the residues in the β tongue. The Cα backbone is colored cyan for the hydrophobic stretch of residues from 177 to 203, and gray for the remainder of the molecule. Side chains within this stretch that are accessible to solvent are colored green (hydrophobic) or blue (hydrophilic); inward-facing side chains are colored in red, with glycines represented by the appropriate hydrogen atom. Two additional hydrophobic side chains, Phe-50 and Val-218, which border this region, are also shown. Panels (A) and (B) were produced using GRASP (Nicholls et al., 1993), and (C) using MIDAS. (Ferrin et al., 1988).

interaction with the bilayer cannot at present be determined. Nevertheless, the evidence from the high-resolution structure of the water-soluble form and the evidence from the pores visualized by electron microscopy enable us to propose essential features of a model for the pore that can be tested by further experiment.

As discussed above, the obvious structural candidate for a transmembrane region in the HlyE structure is the large 30 Å deep hydrophobic patch around the β tongue. Not only is this situated at one end of the molecule, in harmony with the side views from the electron microscopy, but is also consistent with our mutagenic results on the β tongue described earlier. The hydrophobic β tongue presents a smooth exterior profile and is sufficiently extensive to interact with a lipid bilayer, as shown schematically in Figure 5A. The remainder of the surface of the head domain is hydrophilic, so that the entire subdomain, rather than the individual secondary structure elements that comprise it, is amphipathic. Its assignment as the transmembrane region allows the proposal of a simple model for pore formation that does not involve drastic structural rearrangements of the toxin.

In our model of the pore, we propose that the flat face of the β tongue will interact with hydrophobic lipid tails (Figure 5A). This would leave the rest of the head subdomain excellently positioned both to form the hydrophilic lining of the pore itself and to make hydrophilic contacts with other subunits in an annular assembly with a channel through its center (Figures 5B and 5C). Hydrophilic groups above and below the β tongue would be correctly separated to interact with lipid head groups. It has been observed that aromatic side chains are often found at the membrane:solvent interface in membrane–associated proteins (Kreusch et al., 1994), and it is therefore of interest to note that such a pattern is seen in this region of HlyE, with tyrosines 178 and 196 situated at the upper end of the β tongue and Phe-50 below it (Figure 4C).

In order to obtain a cylindrical assembly like that seen in the electron microscopy, a relatively minor conformational change in which the main body of the molecule

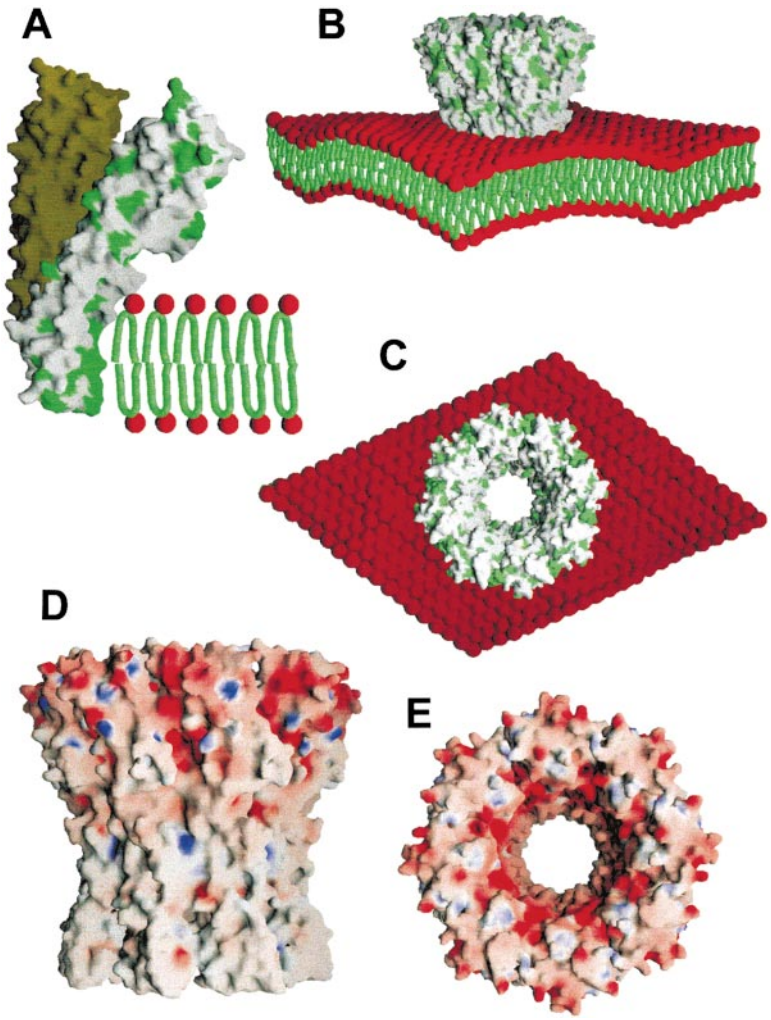

Figure 5. Proposed Models for Membrane Interaction and Pore Formation

Schematic diagrams of HlyE drawn and colored as in Figure 4B interacting with models of a lipid bilayer (head groups shown as red spheres, tails as green worms). The hydrophobic part of the membrane is 30 Å thick in this model. (A) the proposed interaction of the main hydrophobic patch of the head domain (lower right) of an HlyE monomer with the lipid bilayer; a model in which the main body of the molecule is reoriented by approximately 20° with respect to the head domain is shown in dark green. The latter model was used to generate an octameric assembly, which is shown viewed parallel to the membrane plane in (B) and perpendicular to it in (C). (D) and (E) show the electrostatic surfaces of the octameric assembly in views similar to (B) and (C), respectively (red corresponds to a surface potential of less than −30 kcal/[mol · electron], blue to a potential greater than +30 kcal/[mol · electron]). This figure was produced using GRASP (Nicholls et al., 1993).

reorients itself with respect to the head subdomain by approximately 20° would be desirable (Figure 5A). This is plausible as there are few interactions between the head subdomain and the remainder of the molecule, and there are exposed, slightly disordered turns at the beginning (residue 161) and at the end (residue 204) of the subdomain that would be ideally situated to facilitate such a structural rearrangement. This slight reorientation of the head subdomain is comparable with domain movements observed in other toxins such as aerolysin (Parker et al., 1996) and pneumolysin (Gilbert et al., 1999). Simple geometric considerations show that an ensemble of approximately eight HlyE monomers packed together and interacting with the membrane in this manner would be sufficient to form an assembly of the correct dimensions. Thus, modeling an octameric pore produces an assembly (Figures 5B and 5C) whose height including the transmembrane region is 100 Å and whose external diameter varies between 70 and 110 Å, in reasonable agreement with the electron microscopy. The model of the assembly contains a pore whose diameter is 70 Å at its widest point but narrowing to 30 Å at its narrowest where the toxin assembly traverses the lipid bilayer. These dimensions are not only in agreement with the electron microscopy data, which give a mean value of 50 Å for the pore inner diameter, but also with the biophysical measurements of a limiting pore size of 25–30 Å (Ludwig et al., 1995, 1999; Oscarsson et al., 1999). In the model of the oligomer, the β tongue regions face outward to the lipid bilayer, producing a hydrophobic exterior, but the hydrophilic part of the head subdomain forms the inside of the water-permeable channel. Electrostatic surface calculations show that the surface in the proposed transmembrane region is neutral, while the exposed parts of the exterior have an overall slight negative charge (Figure 5D) and the interior of the pore has a relatively strong negative charge (Figure 5E). The last observation is in good agreement with the characterization of the pore as moderately cation selective (Ludwig et al., 1995, 1999).

The model presented here is a conservative one that assumes no major structural rearrangements of the protein and is consistent with the crystallographic, electron microscopy, and mutagenic data. However, it does propose a novel mode of membrane interaction that is quite distinct from those previously proposed for other toxins and membrane-binding proteins, and therefore other possibilities should be considered. One possibility can be eliminated with some confidence: some toxins, after major conformational changes, form pores constructed

from amphipathic β sheets, which assemble to form porin-like β barrel channels across the membrane (Song et al., 1996; Olson et al., 1999). It is clear that this is most unlikely to occur in HlyE since it contains no alternating hydrophobic/hydrophilic sequences that could form such amphipathic transmembrane β strands.

The five-helix bundle that forms the tail subdomain of the molecule would appear to be a possible candidate for a translocation domain. A variety of all-helical domains are found in a number of toxins, including the pore-forming domain of the insecticidal δ endotoxin from *Bacillus thuringiensis* (Li et al., 1996), the pore forming domain of colicins (Parker et al., 1989; Wiener et al., 1997), and the translocation domain of diphtheria toxin (Choe et al., 1992). These bundles typically consist of amphipathic helices packed around a central hydrophobic helix that is thought to become "unsheathed" and inserted into the membrane (Parker and Pattus, 1993). However, this mechanism is unlikely to be employed by HlyE because all the helices are amphipathic. However, a buried hydrophobic helix does not appear to be obligatory: in the translocation domain of *Pseudomonas aeruginosa* exotoxin A (Allured et al., 1986), there is no hydrophobic helix, and it is believed that the helices proceed through a molten globule state in order to present their hydrophobic faces to the lipid during translocation through the membrane, and it is therefore possible that the tail subdomain may have a role to play in translocation of HlyE out of the bacterium, although this must be a topic for future investigations.

Conclusions

The structure of HlyE reveals the architecture of a novel family of toxins. The molecule possesses an extended rod-like structure capped by an amphipathic head domain, in which a predicted transmembrane helix sequence is not a helix but is instead located in a helix-β hairpin-helix structure that creates a hydrophobic patch on the surface of the toxin. Our observations by electron microscopy show that the toxin molecules oligomerize to form channels that project from the membrane and have allowed us to construct a provisional model for the pore itself. In this model, the evidence from mutagenesis, electron microscopy, the crystal structure, and model-building studies indicates that it is the β tongue structure in the head domain that is involved in interaction with the membrane in pore formation. However, many intriguing questions remain. Foremost among them, answerable only by further extensive biochemical, biophysical, and structural studies, are a full description of the mechanism of incorporation of the toxin into the membrane and a detailed, high-resolution structural description of the transmembrane pore assembly.

Experimental Procedures

Purification of HlyE

The *hlyE* coding region was isolated by PCR and cloned into pGEX-KG, allowing IPTG-inducible expression of a GST-HlyE fusion protein containing a thrombin cleavage site. Automated DNA sequencing indicated that the cloned *hlyE* gene sequence was identical to that reported in the complete *E. coli* genome sequence, except for a C to T substitution that results in the substitution of A187 by V and the T2A substitution resulting from an engineered NcoI restriction site used to facilitate cloning. The GST-HlyE fusion protein was isolated by chromatography on GSH-Sepharose 4B, and HlyE was released by thrombin cleavage. As a consequence of the HlyE overproduction and isolation strategy, the final product contains 15 additional N-terminal amino acids (GSPGISGGGGGILDS), the presence of which was confirmed by amino acid sequencing. Prior to crystallization, HlyE was concentrated to approximately 10 mg/ml using Centricon 3 filtration cells (Amicon). Details of the purification and properties of the isolated protein will be reported elsewhere.

Hemolytic activity was measured as described (Rowe and Welch, 1994). The metal-ion content of HlyE was determined by ICP-MS (induced coupled plasma-mass spectrometry) on redissolved freeze-dried samples of HlyE protein. Native molecular weights were estimated on a calibrated Sepharose 6B column (300 mm × 15 mm) equilibrated with Tris-HCl, 25 mM, pH 6.8, containing 100 mM NaCl. The AlteredSites II system (Promega) was used to create the HlyE variants. The proportion of HlyE that acquired an intramolecular disulfide after treatment with diamide (1 mM, 30 min at 37°C) was determined by densitometric analysis of immunoblots from nonreducing SDS-polyacrylamide gels.

Sequences

Preliminary *S. typhi hlyE* sequence data were obtained from the Institute for Genomic Research website at http://www.tigr.org and is designated gnl/Sanger 601S.typhi 316. The *hlyE* gene from *Shigella flexneri* ATCC 12022 was isolated by PCR amplification. Chromosomal DNA was obtained using standard methodologies, and the *hlyE* gene was amplified with Pwo polymerase and two primers homologous to the 5′ and 3′ ends of the *E. coli hlyE*. The sequencing of the PCR product was determined by automated cycle sequencing. The sequence has been deposited in GenBank as entry AF200955.

Crystallization of HlyE

HlyE isolated from the GST-HlyE fusion protein was crystallized by the hanging-drop vapor-diffusion method. This protein consists of the entire HlyE sequence preceded by a 15-residue linker sequence, as confirmed by N-terminal amino acid sequencing of redissolved crystals. For the crystal used for 2.0 Å data collection, the drop consisted of 2 μl 10 mg/ml protein solution in 25 mM Tris HCl buffer at pH 6.8, 100 mM NaCl, and 2.5 mM $CaCl_2$, plus 2 μl of well solution. The well solution (1 ml) consisted of 1.1 M ammonium sulfate and 10 mM $CoCl_2$ in 100 mM MES buffer at pH 6.5. The crystals have the form of flattened tetragonal bipyramids and were found to be in one of the enantiomeric spacegroups $P4_12_12$ or $P4_32_12$, with cell dimensions a = b = 87.4 Å, c = 143.6 Å. At room temperature the crystals diffract to 2.6 Å resolution, but under cryogenic conditions the cell dimensions change to a = b = 84.5 Å, c = 142.7 Å and diffract to at least 2.0 Å on the CCLRC Daresbury Synchrotron Radiation Source.

Data Collection

Two incomplete data sets to 3.0 Å and 2.5 Å, respectively, were collected at room temperature on Stations 9.5 and 9.6, respectively, at the CCLRC Daresbury SRS (Table 1A). These were scaled together (mean fractional isomorphous difference 5.3%) to form one 92% complete data set to a maximum resolution of 2.56 Å. Heavy atom derivatives of HlyE were prepared by soaking native HlyE crystals for up to 15 hr in 1 mM heavy atom compounds dissolved in a modified crystallization buffer (1.5 M ammonium sulfate, 100 mM MES buffer at pH 6, 10 mM $CoCl_2$).

For the high-resolution data collection, a crystal of HlyE, prepared as above, was frozen under a nitrogen stream at 100 K in a cryoprotectant solution consisting of 1.6 M ammonium sulfate, 25% glycerol, 10 mM $CoCl_2$, and 100 mM MES buffer at pH 6.5. Data to 2.0 Å were collected on a MarResearch 345 Image Plate detector on Station PX7.2 at CCLRC Daresbury. Details of data collection are given in Table 1A.

All data sets were processed using the MOSFLM software package (Leslie, 1994) and are summarized in Table 1A. All subsequent crystallographic processing was performed using the CCP4 program suite (Bailey, 1994).

MIR Phasing, Map Calculation, and Density Modification

Heavy atom positions were located from Patterson syntheses. An initial 5 derivative 6.0 Å MIR map showed that the molecule appeared to be an elongated cluster of a helices. Three derivatives were used to calculate the 2.56 Å electron density map, which was of good quality. Details are given in Table 1A. Heavy atom refinements and map calculations were conducted in the two possible enantiomeric spacegroups, $P4_12_12$ and $P4_32_12$. The latter map showed correctly handed α helices and correct L amino acid configurations, and $P4_32_12$ was therefore identified as the correct spacegroup. The MIR map was further improved by flattening the solvent density region using the DM program (Bailey, 1994), during which procedure the DM R_{free} fell from 0.55 to 0.35.

Model Building and Refinement

Rebuilding and Refinement Cycles at 2.56 Å Resolution

The MIR/DM 2.56 Å electron density map was of generally good quality. Over five rounds of refinement using REFMAC (Bailey, 1994; Murshudov et al., 1996) and rebuilding using O (Jones et al., 1991) and FRODO (Jones, 1985) a 97% complete model was built, with good geometry.

Refinement at 2.0 Å Resolution

The 2.56 Å model of the structure of HlyE was refined to 2.0 Å using data collected from a crystal frozen at 100 K. The initial refinement was performed using rigid body refinement in REFMAC (Murshudov et al., 1996), followed by positional refinement with lightly restrained individual B factors. In REFMAC, an overall anisotropic scale was applied between F_{calc} and F_{obs}, and a 2-gaussian bulk solvent correction was used (Tronrud, 1997). Several rounds of refinement, rebuilding, and addition of solvent structure were performed. Details of the final model are given in Table 1B. The final model is complete except for the first 10 residues of the 15-residue linker at the N-terminal, and the five C-terminal residues, all of which are invisible in the otherwise excellent electron density maps (Figure 2E). Twenty side chains are disordered or partially disordered. A total of 339 water molecules and one sulfate group are included in the model. The final overall R factor for the working set was 0.198, with an R_{free} of 0.252, with good geometry (see Table 1B).

Coordinates

The coordinates have been deposited in the Brookhaven Protein Data Bank with the identifier 1QOY.

Electron Microscopy

Reconstitution Experiments

Five microliters of 10 mg/ml HlyE in TCB (25 mM Tris HCl at pH 7.5, 2.5 mM $CaCl_2$, 100 mM NaCl) was mixed with 10 μl of 4 mg/ml mixed brain lipids (Avanti Polar Lipids) solubilized with 2% w/v n-octyl-β-D-glucopyranoside (Calbiochem) to give a final lipid-to-protein weight ratio of 0.8. The samples were diluted with the hemolysin buffer to give a final protein concentration of 0.5 mg/ml in 100 μl. Reconstitution was performed using 10 mg SM2-Biobeads (Rigaud et al., 1997) and the samples incubated at 4°C. Samples were then periodically examined for the formation of hemolysin pores that appeared after 1–2 weeks at 4°C. Alternatively, if vesicles were preformed as above, but in the absence of HlyE, characteristic clusters of pores were observed within 1 min of addition of 10 μl of 0.4 mg/ml HlyE to 25 μl of preformed lipid vesicles (4 mg/ml lipid) at 37°C.

Electron Microscopy

The results of reconstitution experiments were checked by adsorbing samples on glow discharged carbon-coated copper grids and negative staining with 0.75% (w/v) uranyl formate. Micrographs were recorded at a nominal magnification of 50,000× on a Philips CM100 electron microscope operating at 100 kV.

Acknowledgments

We thank Dr. Arthur J. G. Moir for DNA sequencing and for N-terminal sequencing of HlyE crystals, Lynne Kennedy-Johnson for technical support, and Dr. Thomas Walz for comments on the manuscript. The *S. typhi* sequencing was supported by Wellcome Trust. We thank BBSRC, EPSRC, and the Wellcome Trust for their support. The Krebs Institute is a BBSRC designated Biomolecular Sciences center, and the Krebs Institute Structural Studies group is a member of the BBSRC North of England Structural Biology Centre.

Received September 20, 1999; revised December 1, 1999.

References

Allured, V.S., Collier, R.J., Carroll, S.F., and Mackay, D.B. (1986). Structure of exotoxin A of *Pseudomonas aeruginosa* at 3.0 Å resolution. Proc. Natl. Acad. Sci. USA *83*, 1320–1324.

Bailey, S. (1994). The CCP4 suite—programs for protein crystallography. Acta Crystallogr. D *50*, 760–763.

Barton, G.L. (1993). ALSCRIPT: a tool to format multiple sequence alignments. Protein Eng. *6*, 13–27.

Bauer, M.E., and Welch, R.A. (1996). Characterization of an RTX toxin from enterohemorrhagic *Escherichia coli* 0157:H7. Infect. Immun. *64*, 167–175.

Bernstein, F.C., Koetzle, T.F., Williams, G.J.B., Meyer, E.F.J., Brice, M.D., Rodgers, J.R., Kennard, O., Shimanouchi, M., and Tasumi, M. (1977). The protein data bank: a computer based archival file for macromolecular structures. J. Mol. Biol. *112*, 535–542.

Choe, S., Bennett, M.J., Fujii, G., Curmi, P.M.G., Kantardjieff, K.A., Collier, R.J., and Eisenberg, D. (1992). The crystal structure of diphtheria toxin. Nature *357*, 216–222.

Coote, J.G. (1992). Structural and functional relationships among the RTX toxin determinants of gram-negative bacteria. FEMS Microbiol. Rev. *88*, 137–162.

del Castillo, F.J., Leal, S.C., Moreno, F., and del Castillo, I. (1997). The *Escherichia coli* K-12 *sheA* gene encodes a 34-kDa secreted haemolysin. Mol. Microbiol. *25*, 107–115.

Fernandez, I., Ubach, J., Dulubova, I., Zhang, X.Y., Sudhof, T.C., and Rizo, J. (1998). Three-dimensional structure of an evolutionarily conserved N-terminal domain of syntaxin 1A. Cell *94*, 841–849.

Ferrin, T.E., Huang, C.C., Jarvis, L.E., and Langridge, R. (1988). The MIDAS display system. J. Mol. Graph. *6*, 13–27.

Gilbert, R.J.C., Jimenez, J.L., Chen, S.X., Tickle, I.J., Rossjohn, J., Parker, M., Andrew, P.W., and Saibil, H.R. (1999). Two structural transitions in membrane pore formation by pneumolysin, the pore-forming toxin of *Streptococcus pneumoniae*. Cell *97*, 647–655.

Green, J., and Baldwin, M.L. (1997). HlyX, the FNR homologue of *Actinobacillus pleuropneumoniae*, is a [4Fe-4S]-containing oxygen-responsive transcription regulator that anaerobically activates FNR-dependent class I promoters via an enhanced AR1 contact. Mol. Microbiol. *24*, 593–605.

Grindley, H.M., Artymiuk, P.J., Rice, D.W., and Willett, P. (1993). Identification of tertiary structure resemblance in proteins using a maximal common subgraph isomorphism algorithm. J. Mol. Biol. *229*, 707–721.

Harbury, P.A.B. (1998). Springs and zippers: coiled coils in SNARE-mediated membrane fusion. Structure *6*, 1487–1491.

Harris, N.L., Presnell, S.R., and Cohen, F.E. (1994). 4 Helix bundle diversity in globular proteins. J. Mol. Biol. *236*, 1356–1368.

Jones, T.A. (1985). Interactive computer graphics: FRODO. In Methods in Enzymology, Vol. 115, H.W. Wyckoff, C.H.W. Hirs, and S.N. Timasheff, eds. (Orlando, FL: Academic Press), pp. 157–170.

Jones, T.A., Zou, J.Y., Cowan, S.W., and Kjeldgaard, M. (1991). Improved methods for building protein models in electron density maps and the location of errors in these models. Acta Crystallogr. A *47*, 110–119.

Kreusch, A., Neubuser, A., Schiltz, E., Weckesser, J., and Schulz, G.E. (1994). Structure of the membrane channel porin from *Rhodopseudomonas blastica* at 2 Å resolution. Protein Sci. *3*, 58–63.

Leslie, A.G.W. (1994). MOSFLM. Jt. CCP4 ESF-EACBM Newsl. Protein Crystallogr. *26*.

Li, J., Koni, P.A., and Ellar, D.J. (1996). Structure of the mosquitocidal delta-endotoxin CytB from *Bacillus thuringiensis* sp. *kyushuensis* and implications for membrane pore formation. J. Mol. Biol. *257*, 129–152.

Ludwig, A., Tengel, C., Bauer, S., Bubert, A., Benz, R., Mollenkopf,

H.J., and Goebel, W. (1995). SlyA, a regulatory protein from *Salmonella typhimurium*, induces a haemolytic and pore-forming protein in *Escherichia coli*. Mol. Gen. Genet. *249*, 474–486.

Ludwig, A., Bauer, S., Benz, R., Bergmann, B., and Goebel, W. (1999). Analysis of the SlyA-controlled expression, subcellular localization and pore-forming activity of a 34 kDa haemolysin (ClyA) from *Escherichia coli* K-12. Mol. Microbiol. *31*, 557–567.

Murshudov, G.N., Vagin, A.A., and Dodson, E.J. (1996). Refinement of macromolecular structures by the maximum-likelihood method. Acta Crystallogr. D *53*, 240–255.

Nicholls, A., Bharadwaj, R., and Honig, B. (1993). GRASP—graphical representation and analysis of surface properties. Biophys. J. *64*, A166.

O'Brien, A.D., and Holmes, R.K. (1996). Protein toxins of *Escherichia coli* and *Salmonella typhimurium*. In Escherichia coli and Salmonella typhimurium, F.C. Neidhardt, ed. (Washington D.C.: ASM Press), pp. 2788–2802.

Olson, R., Nariya, H., Yokota, K., Kamio, Y., and Gouaux, E. (1999). Crystal structure of Staphylococcal LukF delineates conformational changes accompanying formation of a transmembrane channel. Nat. Struct. Biol. *5*, 134–140.

Oscarsson, J., Mizunoe, Y., Li, L., Lai, L.-H., Wieslander, A., and Uhlin, B.E. (1999). Molecular analysis of the cytolytic protein ClyA (SheA) from *Escherichia coli*. Mol. Microbiol. *32*, 1226–1238.

Oscarsson, J., Mizunoe, Y., Uhlin, B.E., and Haydon, D.J. (1996). Induction of haemolytic activity in *Escherichia coli* by the *slyA* gene product. Mol. Microbiol. *20*, 191–199.

Parker, M.W., Buckley, J.T., Postma, J.P.M., Tucker, A.D., Leonard, K., Pattus, F., and Tsernoglou, D. (1994). Structure of the *Aeromonas* toxin proaerolysin in its water-soluble and membrane-channel states. Nature *367*, 292–295.

Parker, M.W., and Pattus, F. (1993). Rendering a membrane protein soluble in water: a common packing motif in bacterial protoxins. Trends Biochem. Sci. *18*, 391–395.

Parker, M.W., Pattus, F., Tucker, A.D., and Tsernoglou, D. (1989). Structure of the membrane-pore-forming fragment of Colicin-A. Nature *337*, 93–96.

Parker, M.W., vanderGoot, F.G., and Buckley, J.T. (1996). Aerolysin—the ins and outs of a model channel-forming toxin. Mol. Microbiol. *19*, 205–212.

Presnell, S.R., and Cohen, F.E. (1989). Topological distribution of 4-alpha-helix bundles. Proc. Natl. Acad. Sci. USA *86*, 6592–6596.

Ralph, E.T., Guest, J.R., and Green, J. (1998). Altering the anaerobic transcription factor FNR confers a hemolytic phenotype on *Escherichia coli* K12. Proc. Natl. Acad. Sci. USA *95*, 10449–10452.

Reingold, J., Starr, N., Maurer, J., and Lee, M.D. (1999). Identification of a new *Escherichia coli* She haemolysin homolog in avian *E. coli*. Vet. Microbiol. *66*, 125–134.

Rigaud, J.-L., Mosser, G., and Lacapere, J.-J. (1997). Bio-Beads: an efficient strategy for two-dimensional crystallisation of membrane proteins. J. Struct. Biol. *118*, 226–235.

Rossjohn, J., Feil, S.C., McKinstry, W.J., Tweten, R.K., and Parker, M.W. (1997). Structure of a cholesterol-binding, thiol-activated cytolysin and a model of its membrane form. Cell *89*, 685–692.

Rowe, G.E., and Welch, R.A. (1994). Assays of hemolytic toxins. In Methods in Enzymology, Vol. 235, V.L. Clark and P.M. Bavoil, eds. (San Diego, CA: Academic Press), pp. 657–669.

Salyers, A.A., and Whitt, D.D. (1994). Bacterial Pathogenesis: A Molecular Approach (Washington D.C.: ASM Press).

Song, L.Z., Hobaugh, M.R., Shustak, C., Cheley, S., Bayley, H., and Gouaux, J.E. (1996). Structure of staphylococcal alpha-hemolysin, a heptameric transmembrane pore. Science *274*, 1859–1866.

Stanley, P., Packman, L.C., Koronakis, V., and Hughes, C. (1994). Fatty acylation of 2 internal lysine residues required for the toxic activity of *Escherichia coli* hemolysin. Science *266*, 1992–1996.

Sutton, R.B., Fasshauer, D., Jahn, R., and Brunger, A.T. (1998). Crystal structure of a SNARE complex involved in synaptic exocytosis at 2.4 Å resolution. Nature *395*, 347–353.

Tronrud, D.E. (1997). TNT refinement package. In Methods in Enzymology, Vol. 277, C.W.J. Carter and R.M. Sweet, eds. (San Diego, CA: Academic Press), pp. 306–319.

Wiener, M., Freymann, D., Ghosh, P., and Stroud, R.M. (1997). Crystal structure of colicin Ia. Nature *385*, 461–464.

Wilson, I.A., Skehel, J.J., and Wiley, D.C. (1981). Structure of the hemagglutinin membrane glycoprotein of influenza virus at 3 Å resolution. Nature *289*, 366–373.

GenBank Accession Number

The GenBank accession number for the sequence of *Shigella flexneri* HlyE reported in this paper is AF200955.